Fingerprint Matching Based on Global Comprehensive Similarity

Yuliang He[1,2], Jie Tian*[1,2], Senior Member, IEEE, Liang Li [1], Hong Chen[1], Xin Yang[1]

1. Center for Biometrics and Security Research, Key Laboratory of Complex Systems and Intelligence Science, Institute of Automation, Chinese Academy of Science, P.O.Box 2728, Beijing 100080, China

2. Graduate School of the Chinese Academy of Sciences, Beijing 100039, China

tian@doctor.com

http://www.fingerpass.net

Running Title:

Fingerprint Matching Based on Global Comprehensive Similarity

*Correspondence Address:

Jie Tian, Senior member of the IEEE Computer Society

Biometrics Research Group, Key Laboratory of Complex Systems and Intelligence Science,

Institute of Automation, Chinese Academy of Sciences, P.O.Box 2728,

Beijing 100080, China

E-mail: tian@doctor.com

http://www.fingerpass.net

Tel: 8610-62532105

Fax: 8610-62527995

Abstract

This paper introduces a novel algorithm based on global comprehensive similarity with three steps. To describe the Euclidean space–based relative features among minutiae, we first build a minutia-simplex that contains a pair of minutiae as well as their associated textures, with its transformation-variant and invariant relative features employed for the comprehensive similarity measurement and parameter estimation respectively. By the second step, we use the ridge-based nearest neighbourhood among minutiae to represent the ridge-based relative features among minutiae. With these ridge-based relative features, minutiae are grouped according to their affinity with a ridge. The Euclidean space-based and ridge-based relative features among minutiae reinforce each other in the representation of a fingerprint. Finally, we model the relationship between transformation and the comprehensive similarity between two fingerprints in terms of histogram for initial parameter estimation. Through these steps, our experiment shows that the method mentioned above is both effective and suitable for limited memory AFIS owing to its less than 1k byte template size.

Key words: Fingerprint identification; ridge-based nearest neighbourhood among minutiae; relative feature; minutia-simplex

1. Introduction

A fingerprint is a pattern of ridges and valleys on the surface of a finger. It has been used for individual identification for legal purposes. Automatic fingerprint identification, which is established on modern information technology, is even applied to civilian purposes such as access control, financial security and verification of firearm purchasers. In fact, the Automatic Fingerprint Identification Systems (AFISs) have been performed well for years in controllable circumstances. However, limited fingerprint quality, non-linear distortion, limited time and memory expense in an off-line AFIS, such as Personal Digital Assistant (PDA) and IC Card systems, are still challenging tasks in fingerprint matching.

This paper introduces an identification algorithm based on global comprehensive similarity with the view to overcome the dilemmas encountered in fingerprint matching process. The new method introduces minutiae and local ridge information in fingerprint representation. Local ridge information helps to represent a local fingerprint region and prevent matching from failing for insufficient minutiae. A minutia-simplex is built to describe a 2nd order Euclidean space-based relative structure [1] between two minutiae, and all minutia-simplexes that closely connect minutiae and ridges represent a fingerprint. So a fingerprint is understood to be composed of many local regions, each of which is represented by one or more minutia-simplexes. If a fingerprint region deforms very little, the relative features of minutiae can be aligned for matching by using rigid transformation. Two minutiae of a minutia-simplex are subject to the positional constraint. Among other relative structures, such as minutia-triplet [2][3], it has more reliable performance in fingerprint matching because of its rich relative features. Compared with minutia-triplet [2][3], however, minutia-simplex has better trade-off between its performance and computational expense. It is known that Euclidean-space relative structures have their own

3

limitation in fingerprint representation. For example, local texture of two relative structures is different though their relative features are similar. Therefore, ridge-based nearest neighbourhood among minutiae is introduced to represent ridge-based relative features with ridge-counts between ridges and minutiae. And minutiae are connected as a topological network with ridges. The ridge-based and Euclidean-space relative features reinforce each other in fingerprint representation. As compared with ridge-counts among minutiae in methods [2][4], the ridge-based nearest neighbourhood among minutiae is more reliably detected although they may be influenced by outlier rejection.

In fingerprint matching, local comprehensive similarity and local transformation parameter are first obtained by coarsely matching between relative structures. Then, the relationship between the comprehensive similarity and transformation is modeled in terms of histogram for calculating an initial transformation model. Finally, the variable bounded box method [5] is used for double-checking local comprehensive similarities. Both the histogram and variable bounded box methods globally reduce the influence of deformation on matching. For uncontrollable conditions, such as large-deformations and large-area outlier rejection, histogram and variable bounded box may be affected and as a consequence, their parameters should be aligned accordingly.

This paper is organized as follows: In section 2, we provide an overview of current fingerprint identification methods in literature. As to Sections 3 we try to manifest how our method works in fingerprint reprocessing, fingerprint representation, transformation model analysis and final matching. Section 4 is an objective evaluation of the new method with the experimental results. The last section confirms the value of the proposed method and provides some prospects in the future.

2. A brief overview of fingerprint identification methods

Fingerprint identification involves a wide range of algorithms with different techniques. These schemes are based predominantly on local landmarks, exclusive global features as well as comprehensive fingerprint features [6]. The minutiae-based matching methods, such as Jiang's and Bhanu's matching and indexing methods using minutiae-triplets [2][3] and Gold's graph matching method [4], locate minutiae, match their relative placement in an input fingerprint and a template. The minutiae-based technique is widely used because it takes less memory expense and has time saving advantages. However, a minutia set cannot characterize overall pattern of a fingerprint, and a minutiae-based fingerprint matching system can hardly match two fingerprints containing different number of unregistered minutiae. And it is hard to further improve their performance.

The exclusive global feature-based techniques are used not only for indexing [7][8] but also for identification [9][10][11][12]. They match the global patterns of the fingerprint texture by aligning the input global features and measuring the maximum mutual global information between two fingerprints. In these methods, however, the central point should be determined with a reliable accuracy and it is difficult to deal with distortion in the fingerprints. The exclusive global information-based AFISs also need more memory to store a fingerprint template than the other two kinds of AFISs.

Comprehensive feature-based techniques [13][14][15] are also seen as a hybrid matching method by fusing minutiae, local features and global features. Local features help accelerate the alignment of the unregistered minutia patterns in different sizes. Global features are used to overcome the shortage of minutiae and local features in bad quality fingerprints. With the reasonable time and memory expenses, comprehensive feature-based techniques outperform two aforementioned kinds of matching methods. Additionally, they combine various classifiers for

fingerprint matching. With the advanced hardware technology, these approaches have become popular for their good performance in acceptable memory expense in recent years.

These methods work well for the controllable environment of small deformation and small-area outlier rejection, while they are not omnipotent methods which robustly perform with some special conditions with large-deformation.

3. Fingerprint matching technique based on global comprehensive similarity

The method is a comprehensive feature-based technique with two novel aspects: First, a minutia-simplex and the ridge-based nearest neighbourhood among minutiae are combined to represent the relative features among minutiae. Second, improved from our previous work [16] in alignment, the relationship between the comprehensive similarity and transformation is a model in terms of histogram for estimating an initial mapping model. Compared with our previous work [16] in alignment, the new method has two novel points: local similarity is checked with ridge-based relative features, and the estimated parameter is only used as an initial one.

3.1. Fingerprint pre-processing

With our method, fingerprint features are extracted from a thinned fingerprint for two reasons: first, it contains enough information to represent the uniqueness of a fingerprint. Second, in the thinned fingerprint, minutiae are more accurately detected and ridges are more efficiently tracked than its corresponding grey fingerprint. Generally, a thinned fingerprint is obtained from a serial of steps including normalization, enhancement, binarization, thining, and post-processing [17][18] . Cheng's dyadic scale space-based fingerprint enhancement method [19] has been applied in our AFIS for a fingerprint is often affected by multi-spectrum noises. In this method, a fingerprint can be divided into a series of scale spaces with its corresponding Gaussian filter for the enhancement. The combined statistical and structural approach [18] and knowledge-based

enhancement method [17] have been employed in our AFIS to binarize and post-process the en-hanced fingerprint.   The fingerprint pre-processing in our AFIS is displayed in Figure 1, where Figure 1-a is from the first fingerprint database (DB1_a) of the 1st International Fingerprint Veri-fication Competition in 2000 (FVC2000) [20]; Figures 1-b to1-d indicate the corresponding ori-entation image, binary image and thinned image respectively.

a   b
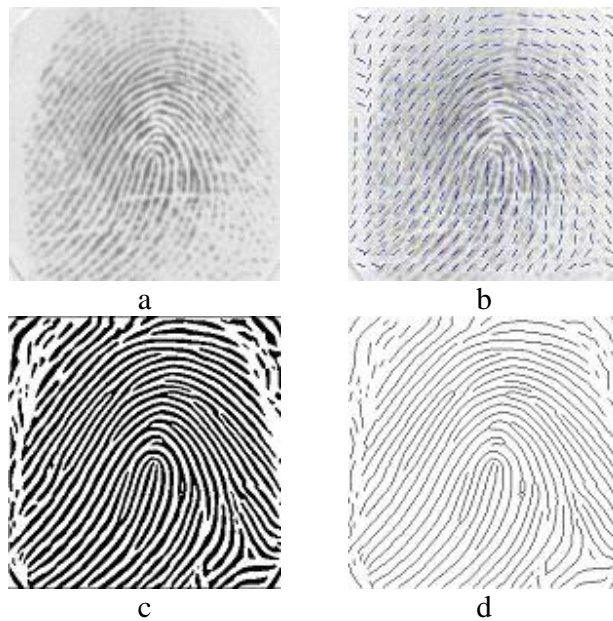
c   d

Figure 1. Fingerprint pre-processing with our AFIS.   a: an original fingerprint in DB1_a of FVC2000; b: its block orientation field; c: enhanced one; d: thinned one

3.2. Fingerprint representation in our method

The uniqueness of a fingerprint is determined by topographic pattern of its texture structure and certain ridge anomalies termed as minutiae.   A challenging task of a fingerprint matching method is to extract enough reliable features in a small memory expense.   Nowadays, compre-hensive features combining minutiae and ridge information have been widely used in matching and they have been performing well.   However, the proposed technique includes the various texture-based features as part of the minutiae-simplex and finds fingerprint alignment.   The ridge-based nearest neighbourhood among minutiae is used as a feature to demonstrate the ridge-

based relative relations among minutiae.   This technique combines the Euclidian space-based and ridge-based relative features.   In this section, comprehensive minutiae and their Euclidian-based and ridge-based relative features will be proposed to characterize the uniqueness of a fingerprint.

3.2.1. Comprehensive minutiae

A fingerprint of bad quality may be too dry, too wet or the foreground area may be so narrow that no enough reliable minutiae can be detected.   In some cases, two fingerprints even from the same finger fail to match for lack of common minutiae.   Therefore, minutiae and associated ridge information are combined in proposed method to improve fingerprint representation.

Vector set $M^F = \{M^F_i = (x^F_i, y^F_i, \alpha^F_i, \beta^F_i, \varphi^F_{i1,...}, \varphi^F_{iT}, d^F_{i1}, ..., d^F_{iT}); |M^F| \geq i \geq 1, T \geq 2\}$ denotes all comprehensive minutiae in fingerprint F, where $|M^F|$ is the number of the minutiae in fingerprint F and T denotes the number of sampled points along a ridge skeleton associated with a minutia. M^F_i, the ith minutia, see Figure 2, is denoted by a feature vector $(x^F_i, y^F_i, \alpha^F_i, \beta^F_i, \varphi^F_{i1,...}, \varphi^F_{iT}, d^F_{i1}, ..., d^F_{iT})$ ($|M^F| \geq i \geq 1, T \geq 2$), where: 1) x^F_i and y^F_i denote its coordinates; 2) α^F_i denotes its orientation, the angle from the horizontal axis OX to its local ridge direction in the anticlockwise direction; 3) β^F_i denotes the local grey variance of a 16×16 area centered by M^F_i; 4) φ^F_{ik} and d^F_{ik} ($|M^F| \geq i \geq 1, T \geq k \geq 1$) respectively denote the direction and distance from M^F_i to the kth point sampled along the ridge skeleton beginning at M^F_i in the equal step.   And the equal step is a constant pixel count between two adjacent sampled points along the skeleton. And it is set to three times the ridge width in our study. φ^F_{ik} and d^F_{ik} are determined by k^{th} sampled point on the ridge associated with M^F_i.   Therefore, φ^F_{ik} and d^F_{ik} will be affected by spurs or kinks in the skeleton.   To reduce their effect on φ^F_{ik} and d^F_{ik}, Luo's knowledge-based post-processing method [17] is used to smooth fingerprint skeleton after thinning.

All φ^F_{ik} and d^F_{ik} are employed to describe the ridge information associated with M^F_i. β^F_i, φ^F_{ik} and d^F_{ik} ($|M^F| \geq i \geq 1$, $T \geq k \geq 1$) are combined to describe local texture and ridge information of the local region associated with M^F_i respectively. These features help align and distinguish input features in matching.
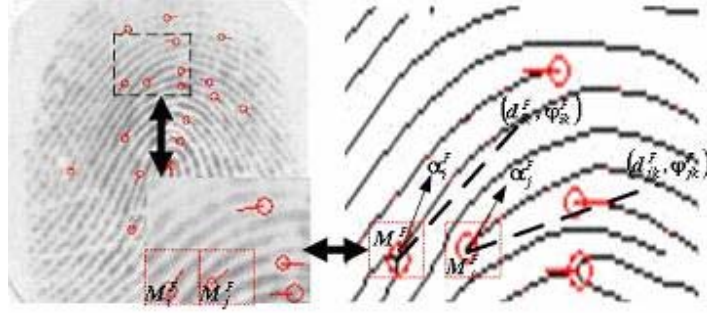

Figure 2. Minutiae and their associated local ridge information

3.2.2. Relative structures among minutiae

In fingerprint analysis, minutiae are more abstract than fingerprint pixels. They are related to each other and attributed by (unary) properties. In other words, a fingerprint can be simply represented by minutiae constrained with their properties and relations. It is the bilateral or higher order relations that convey the contextual constraints. They play a crucial role in fingerprint matching. In this algorithm, two relative structures among minutiae are introduced as minutia-simplex and ridge-based nearest neighbourhood among minutiae.

A. Minutia-simplex

n^{th} ($n \geq 1$) order relative structures among minutiae combine all comprehensive minutiae as a whole. These relative structures are usually classified into unary minutia, minutia-simplex, and minutia-triplet. Minutiae have seldom been used as unary relative structures because they do not have relative features to globally represent a fingerprint. 3rd order relative structures, such as minutia-triplet employed in many methods [2][3], require more computational expense though

they have more robust performance in matching.   2nd order relative structures also have enough relative features and keep a good trade-off between computational expense and performance. Therefore, minutia-simplex, 2nd order relative structure of minutiae is proposed in our study, as shown in Figure 3.

Let $E^F=\{E^F_i=(p^F_i,\ q^F_i,\ l^F_i,\ \theta^F_i,\ u^F_i,\ v^F_i);\ |E^F|\geq i\geq 1\}$ denote the minutia-simplex set of fingerprint F, where: 1) $|E^F|$ is the size of the minutia-simplex set.   2) p^F_i and q^F_i ($|M^F|\geq p^F_i,\ q^F_i\geq 1$) denote the serial numbers in the minutia set M^F. $M^F_{p_i}$ and $M^F_{q_i}$ are two ending minutiae of a minutia-simplex E^F_i when $L_h\geq\left\|\left(x^F_{p_i},y^F_{p_i}\right)\ \left(x^F_{q_i},y^F_{q_i}\right)\right\|_2\geq L_l$, where L_l and L_h are the lower and upper bounds of the length of a valid minutia-simplex respectively; $\left(x^F_{p_i},y^F_{p_i}\right)$ and $\left(x^F_{q_i},y^F_{q_i}\right)$ are the coordinates of $M^F_{p_i}$ and $M^F_{q_i}$ respectively.   Assume that the local region centred by M^F_i deforms very little, the relative features of all minutia-simplexes associated with M^F_i can be linearly transformed in this local region. 3) $l^F_i=\left\|\left(x^F_{p_i},y^F_{p_i}\right)\ \left(x^F_{q_i},y^F_{q_i}\right)\right\|_2$ and denotes the length of the minutia-simplex.   4) $\theta^F_i=\arctan\left(\dfrac{x^F_{p_i}-x^F_{q_i}}{y^F_{p_i}-y^F_{q_i}}\right)$ denotes the direction of the minutia-simplex.   5) $u^F_i=\alpha^F_{p_i}-\theta^F_i$ and $v^F_i=\alpha^F_{q_i}-\theta^F_i$.   They are derivative relative features of minutia-simplex E^F_i, respectively denoting its directional differences away from $\alpha^F_{p_i}$ and $\alpha^F_{q_i}$.

Relative features of a minutia-simplex are divided into two parts, transformation-invariants and transformation-variants, which are used for local similarity measurement and alignment respectively.   Transformation-invariants l^F_i, u^F_i and v^F_i are irrelevant with linear transformation, such as translation and rotation, and can be used for direct similarity measurement if scaling is not considered.   Transformation-variant ^F_i changes with rotation and is used to model rotating

input minutiae referred to the template. The size of set E^F, $|E^F|$, is determined by thresholds L_l

and L_h. $|E^F|$ is much less than $\binom{|M^F|}{2}$ because the distances between many minutia pairs are

beyond the interval $[L_l, L_h]$. For each minutia, thresholds L_l and L_h are used to set a circular

region in a minimum deformation, and geometric transformation of a minutia simplex is assumed

to be linear. That is, the direction of a minutia-simplex in the local region is in linear relation

with fingerprint rotation parameter. In the proposed method, L_l and L_h are set to five and fifteen

times ridge-width respectively, see Appendix.

B. Ridge-based nearest neighbourhood among minutiae

Like a minutia-triplet, a minutia-simplex only describes the Euclidean space-based relative fea-

tures among minutiae. These relative structures can not completely explain the complex local

texture and results in mismatch. For example, minutia-simplex pair (M^F_i, M^F_j) and $(M^G_{i'}, M^G_{j'})$

in Figure 4 is mismatched because their relative features are very similar. However, it is easier

to distinguish the minutia-simplex (M^F_i, M^F_j) from the minutia-simplex $(M^G_{i'}, M^G_{j'})$ with their

ridge-based relative features.

Let R^F_i ($|M^F| \geq i \geq 1$) denote the ridge beginning at M^F_i and r^F_{ij} the ridge-count between M^F_j and

the ridge R^F_i. Set $\{r^F_{ij} \mid i; |M^F| \geq j \geq 1\}$ denotes the ridge-based nearest neighbourhood of M^F_i and

describes the ridge-based relative features among M^F_i and other minutiae. r^F_{ij} is more easily

detected than ridge-count between two minutiae used in method [2]. In our study, r^F_{ij} is set to 0

or 1 or 2 in three cases respectively: (1) $r^F_{ij} = 0$ when M^F_i and M^F_j are on the same ridge R^F_i, such

as M_1 and M_2 in Figure 5; (2) $r^F_{ij} = 1$ when there is no more than one ridge between M^F_j and R^F_i,

like M_4 and M_5 in Figure 5; (3) $r^F_{ij} = 2$ when M^F_i and M^F_j meet neither condition (1) nor (2), such

as M_3 and M_6 in Figure 5.   The ridge-based nearest neighbourhood among minutiae describes the novel ridge-based relative features among minutiae.

3.3. Transformation parameter analysis

For a randomly-placed finger, it is necessary to align input minutiae to the template during matching.   The alignment generally includes rotation, translation, and shearing.   The alignment significantly affects the comprehensive similarity of two fingerprints.   A transformation model also needs to be optimized to obtain the maximal comprehensive similarity.   However, it is difficult to estimate the maximal comprehensive similarity if one doesn't know the optimal transformation model.   In our study, the relationship between the comprehensive similarity and transformation model was built for estimating an optimal transformation model.   The model is confirmed effective by our experimental result.

This matching algorithm is designed assuming that input and template fingerprints are captured with the same device but with little scaling deformation under the same condition.   Since fingerprint matching performs well in polar coordinate, translation of the input features to the template is not used if the central point is set in advance.   So one of the most important tasks in alignment is to obtain the optimal rotation parameter.

3.3.1. Local comprehensive similarity measurement

In some matching methods, such as Jiang's local and global structure based minutiae matching method [2], local similarities between relative structures are accumulated to calculate the global similarity.   In our study, local similarities are also used for estimating transformation-parameters, and they are calculated by coarsely comparing transformation-invariant relative features of minutiae-simplexes.
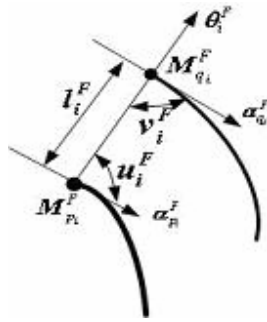
Figure 3. Minutia-simplex E^F_i. Minutiae $M^F_{p_i}$ and $M^F_{q_i}$ are its two ending points; l^F_i, θ^F_i, u^F_i, and v^F_i are its relative features.
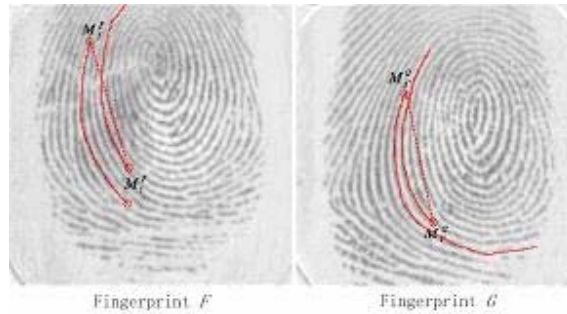

Fingerprint F Fingerprint G

Figure 4. Differences between ridge-based relative features. The ridge-based nearest neighbourhood of M^F_i and M^F_j is obviously dissimilar to that of $M^G_{i'}$ and $M^G_{j'}$ though their Euclidean space-based relative features are similar.
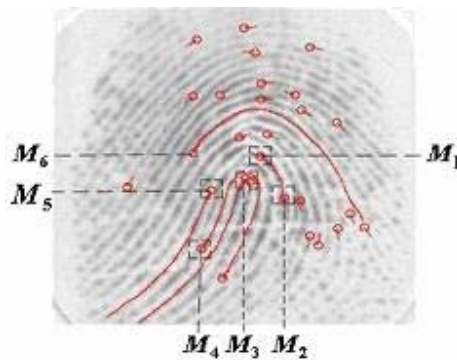

Figure 5. Ridge-based nearest neighbourhood among minutiae. (1) M_1 and M_2 are located on the same ridge; (2) There is no more than one ridge between M_4 and ridge R_5 beginning at M_5; (3) M_3 and M_6 meet neither condition (1) nor (2).

Set $S = \{(S_{ij}, I_{ij}); S_{ij} \geq 0, I_{ij} = 0$ or $1, |E^F| \geq i \geq 1, |E^G| \geq j \geq 1\}$ denote all local comprehensive similarities between two minutia-simplex sets E^F and E^G, where S_{ij} is the local similarity between E^F_i and E^G_j, and I_{ij} is their matching order. If $I_{ij} = 1$, E^F_i and E^G_j are assumed to be matched in positive order; otherwise, in reverse order.

$$\begin{cases} I_{ij} = \left(S_{ij}^{(0)} < S_{ij}^{(1)} \right) \\ S_{ij} = \max\left\{ S_{ij}^{(0)}, \ S_{ij}^{(1)} \right\} \end{cases} \tag{1}$$

, where the similarity measurement function f, $S_{ij}^{(0)}$, and $S_{ij}^{(1)}$ are defined as

$$\begin{cases} S_{ij}^{(0)} = f\left(\Delta, diff_0\left(\left(E_i^F, M_{p_i}^F, M_{q_i}^F \right), \left(E_j^G, M_{q_j}^G, M_{p_j}^G \right) \right) \right) \\ S_{ij}^{(1)} = f\left(\Delta, diff_1\left(\left(E_i^F, M_{p_i}^F, M_{q_i}^F \right), \left(E_j^G, M_{p_j}^G, M_{q_j}^G \right) \right) \right) \\ f\left((\Delta_1, ..., \Delta_n), (x_1, ..., x_n) \right) = \frac{1}{n} \sum_{k=1}^{n} \frac{\|\Delta_k - x_k\|}{\|\Delta_k\|} \end{cases} \tag{2}$$

In Formula (2), $\Delta = \left(\Delta_l, \Delta_\beta, \Delta_\beta, \Delta_\alpha, \Delta_\alpha, \Delta_l, ..., \Delta_l \right)$, and $diff_0\left(\left(E_i^F, M_{p_i}^F, M_{q_i}^F \right), \left(E_j^G, M_{p_j}^G, M_{q_j}^G \right) \right)$ and $diff_1\left(\left(E_i^F, M_{p_i}^F, M_{q_i}^F \right), \left(E_j^G, M_{p_j}^G, M_{q_j}^G \right) \right)$ are defined as

$$\begin{cases} diff_1\left(\left(E_i^F, M_{p_i}^F, M_{q_i}^F \right), \left(E_j^G, M_{p_j}^G, M_{q_j}^G \right) \right) = \begin{pmatrix} l_i^F - l_j^G, \beta_{p_i}^F - \beta_{p_j}^G, \beta_{q_i}^F - \beta_{q_j}^G, u_i^F - u_j^G, v_i^F - v_j^G, \\ d_{p_i 1}^F - d_{p_j 1}^G, ..., d_{p_i T}^F - d_{p_j T}^G, d_{q_i 1}^F - d_{q_j 1}^G, ..., d_{q_i T}^F - d_{q_j T}^G \end{pmatrix} \\ diff_0\left(\left(E_i^F, M_{p_i}^F, M_{q_i}^F \right), \left(E_j^G, M_{q_j}^G, M_{p_j}^G \right) \right) = \begin{pmatrix} l_i^F - l_j^G, \beta_{p_i}^F - \beta_{q_j}^G, \beta_{q_i}^F - \beta_{p_j}^G, u_i^F - u_j^G - 180^\circ, v_i^F - v_j^G \ 180^\circ, \\ d_{p_i 1}^F - d_{q_j 1}^G, ..., d_{p_i T}^F - d_{q_j T}^G, d_{q_i k}^F - d_{p_j k}^G, ..., d_{q_i T}^F - d_{p_j T}^G \end{pmatrix} \end{cases} \tag{3}$$

In Formula (3), Δ_l, Δ_α, and Δ_β denote the error thresholds of distance, direction and grey variance of a minutia-simplex respectively. They are estimated from training datasets and set to 16 pixels, 10°, 16 respectively, see Appendix. $diff_1\left(\left(E_i^F, M_{p_i}^F, M_{q_i}^F \right), \left(E_j^G, M_{p_j}^G, M_{q_j}^G \right) \right)$ is produced by matching the transformation invariant features of $\left(E_i^F, M_{p_i}^F, M_{q_i}^F \right)$ and those of $\left(E_j^G, M_{p_j}^G, M_{q_j}^G \right)$

in positive matching order. $diff_0\left(\left(E_i^F, M_{p_i}^F, M_{q_i}^F\right), \left(E_j^G, M_{q_j}^G, M_{p_j}^G\right)\right)$ is generated by matching the

transformation invariant features of $\left(E_i^F, M_{p_i}^F, M_{q_i}^F\right)$ and those of $\left(E_j^G, M_{q_j}^G, M_{p_j}^G\right)$ in reversed

matching order. And the directional relative features of E_j^G, θ_j^G, u_j^G and v_j^G, are aligned as

$\theta_j^G + 180°, u_j^G + 180°$ and $v_j^G + 180°$ respectively.

Deformation in fingerprints affects the similarity set S and results in mismatch. In our study, the ridge-based nearest neighbourhood among minutiae is used to check all local similarities.

3.3.2. Checking local similarity with ridge-based nearest neighbourhood among minutiae

In local similarity measurement in Formula (1), error thresholds, Δ_l, Δ_α, and Δ_β are used to counteract the influence of spurs on relative features in matching. The scheme of tolerance deviation also results in mismatch. For example, two similar local regions, being from two different fingers, are often mismatched with the Euclidean space-based relative features. In our study, the ridge-based nearest neighbourhood among minutiae is used to overcome the fault by double-checking these coarse matching results to determine local mismatch in Set S.

Each element in set S is mismatch if E_i^F and E_j^G don't meet the condition described in Formula (4), depicting the difference between the ridge-based nearest neighbourhood of minutia pair $\left(M_{p_i}^F, M_{q_i}^F\right)$ and that of minutia pair $\left(M_{p_j}^G, M_{q_j}^G\right)$. If $I_{ij}=1$, indicating E_i^F is matched to E_j^G in positive order, $r_{p_iq_i}^F$ and $r_{q_ip_i}^F$ are compared with $r_{p_jq_j}^G$ and $r_{q_jp_j}^G$ respectively. Vice versa, if $I_{ij}=0$, indicating E_i^F is matched to E_j^G in reverse order, $r_{p_iq_i}^F$ and $r_{q_ip_i}^F$ are compared with $r_{q_jp_j}^G$ and $r_{p_jq_j}^G$ respectively.

$$\begin{cases} \left(\left|r_{p_iq_i}^F - r_{p_jq_j}^G\right| \le 1\right) AND \left(\left|r_{q_ip_i}^F - r_{q_jp_j}^G\right| \le 1\right), & if\ I_{ij}=1 \\ \left(\left|r_{p_iq_i}^F - r_{q_jp_j}^G\right| \le 1\right) AND \left(\left|r_{q_ip_i}^F - r_{p_jq_j}^G\right| \le 1\right), & if\ I_{ij}=0 \end{cases} \qquad (4)$$

3.3.3. Local transformation parameter estimation

Affine transformation model is a feasible and effective model for fingerprint matching [21] and it needs three parameters θ, t_x, and t_y if scaling is not considered in our study. Only the rotation parameter θ is required if center points of two fingerprints are given and matching is done in polar system. Based on the coarse matching results, local rotation parameter measurement is introduced in this section.

Set $\boldsymbol{\theta} = \{\theta_{ij}; |E^F| \geq i \geq 1, |E^G| \geq j \geq 1\}$ denote all local rotation parameters calculated from all local relative structures. In our study, a local rotation parameter is represented by the direction difference between a local relative structure and its corresponding template one, which is based on the assumption that each local fingerprint region deforms very little. Formula (5) uses the mean of local directional biases of an input minutia-simplex referred to its corresponding template one as a local rotation parameter.

$$\theta_{ij} = \frac{1}{2T+2} \left[\sum_{k=1}^{T} \left[\left(\varphi_{p_i k}^F + \varphi_{q_i k}^F \right) - \left(\varphi_{p_j k}^G + \varphi_{q_j k}^G \right) \right] + \left(\alpha_{p_i}^F + \alpha_{q_i}^F \right) - \left(\alpha_{p_j}^G + \alpha_{q_j}^G \right) \right] \tag{5}$$

3.3.4. Modelling the relation between comprehensive similarity and rotation parameter

Many methods, such as Cappelli's plastic distortion model [22], Bazen's thin-plate spline model [23], Senior's equally spaced fingerprint conversion [24], are proposed to model non-linear deformation patterns. However, these methods have their limits in fingerprint identification application systems though they can partially solve deformation under controllable situations. For example, with the plastic distortion model [22], it is hard to obtain enough information to build the deformation model. Senior's equally spaced fingerprint conversion [24] would fail if the compression or traction force is parallel to the local ridge orientation and the inter-ridge space

will not change. Bazen's thin-plate spline model [23] is good at distinguishing the major differences from different fingerprints, however, it is weak in detecting their minor differences.

In this paper, using a series of local relative structures with little local deformation, the distribution of global comprehensive similarity along rotation parameter is modelled to calculate an optimal rotation parameter. In matching, the rotation parameter is adjusted in a small interval to reduce the impact of mismatches in the coarsely matching stage on the global rotation parameter. For local similarity set S and its corresponding local directional bias set θ, their relationship is denoted with a similarity function $H(S, \theta)$ built with Formula (6) in terms of histogram. Figure 7 illustrates $H(S, \theta)$, which comes from coarse results by matching two fingerprints from the same finger, see Figure 6.

$$H(S \quad \theta) = \sum_{i=1}^{\left|E^F\right|} \sum_{j=1}^{\left|E^G\right|} \delta_1(\theta_{ij} - \theta) \times S_{ij} \tag{6}$$

where $\delta_1(x)$ is an impulsive function; if $x=0$, $\delta_1(x) =1$; otherwise, $\delta_1(x) =0$.

Local similarity measurement is disturbed by noises so that $H(S, \theta)$ will be affected accordingly. A filter function, $w(x) = \frac{1}{2}\left[1 - \cos(\frac{x\pi}{d})\right]$ (2d+1≥x≥1), is used to decrease noises in $H(S, \theta)$. Filtered $H(S, \theta)$ is shown in Figure 8. $H(S, \theta)$, a periodical function, can be extended by half a period, which doesn't influence its performance. And the histogram has only one peak in a period, where the rotation parameter is optimal. In our study, the maximum of $H(S, \theta)$ is used to coarsely measure the gobal similarity between fingerprints F and G.

Theoretically, the rotation parameter θ_0, where $H(S, \theta_0)$ is the maximal, is the global optimal one, called as θ_m. It is calculated with geometric mean method as shown in Formula (7) and Figure 9, where is set to less than half of directional error threshold Δ_α, and $\gamma \in (0,1]$ is applied for an confidence interval of the global similarity. They are set to 5 and 0.6677 respectively in

this method. For example, if $H(\boldsymbol{S}, \boldsymbol{\theta})$ is of normal distribution, the confidence of the global similarity is $2\phi\left(\sqrt{-2\ln\gamma}\right)$-1=0.6318 when γ=0.6667. If θ_m is beyond the interval preset for the rotation transformation parameter, this matching fails. In Formula (7), $H(\mathrm{S}, \theta_0)$=max$\{H(\boldsymbol{S}, \boldsymbol{\theta})\}$; $h(x)$=0 if x<0; otherwise, $h(x)$=x.

$$\theta_m = \frac{\sum_{\theta\in[\theta_0-\sigma, \theta_0+\sigma]}\left\{\theta \times h\left(H(S,\theta) - \gamma \times H(S,\theta_0)\right)\right\}}{\sum_{\theta\in[\theta_0-\sigma, \theta_0+\sigma]} h\left(H(S,\theta) - \gamma \times H(S,\theta_0)\right)} \qquad (7)$$

Deformation and large-area outlier rejection will influence on the Euclidean relative features and then affect the on rotation parameter estimation. For general controllable environments of small deformation and small-area outlier rejection, θ_m is aligned in the interval [-1°, +1°] to reduce the influences on the estimation. While under special condition of large-deformation and large-area outlier rejection, θ_m should be aligned in a lager interval and non-rigid parameter estimation will perform better.

3.4. Fingerprint matching

Deformation in fingerprints may bring false local similarities in $\boldsymbol{S}$ and therefore affects the final comprehensive similarity. Thus the global fingerprint matching is essential after the coarse local matching if the transformation model is known. In this section, the variably–sized bounding method [5] is used to double-check all local comprehensive similarities to reduce the influence of deformation in fingerprints. It consists of three steps: setting the center points, aligning the input minutiae to the template, and double-checking all the local similarities.

First, the comprehensive similarity of a pair of minutiae is calculated from local similarity set S, shown in Formula (8). The pair of minutiae with the greatest comprehensive similarity are selected as central points.

$$
\begin{cases}
U_{ij} = \sum\limits_{m=1}^{|E^F|}\sum\limits_{n=1}^{|E^G|}\left[S_{mn}\delta_2\left(p_m^F,q_m^F,p_n^G,q_n^G,i,j,I_{mn}\right)\right]\\[2mm]
\delta_2(x,y,u,v,a,b,\lambda) = \begin{cases}1,\ if\ (a,b)\in\{(x,u),(y,v)\}\wedge(\lambda=1)\\ 1,\ if\ (a,b)\in\{(x,v),(y,u)\}\wedge(\lambda=0)\\ 0,\ otherwise\end{cases}
\end{cases}
\tag{8}
$$

Let $U=\{U_{ij};\ |M^F|\geq i\geq 1,\ |M^G|\geq j\geq 1\}$ denote the set of all comprehensive similarities of minutia

pairs, where U_{ij} is the sum of local similarities of all minutia-simplex pairs in $\{(E^F_m, E^G_n)|((i=$

p^F_m or $q^F_m)$ and $(j=p^G_n$ or $q^G_n))\}$, and denotes the comprehensive similarity between M^F_i and M^G_j.

$(O_F,\ O_G) = \left((x^F_{o_i},y^F_{o_i}),(x^G_{o_j},y^G_{o_j})\right)$ is selected as the center points in alignment, where

$U_{o_i o_j} = \max\limits_{(i,j)}\{U_{ij}\}$ $(|M^F|\geq i,\ o_i\geq 1,\ |M^G|\geq j,\ o_j\geq 1)$. In Formula (8), function δ_2 is used to judge

whether a minutia-simplex pair is associated with the minutia pair (M^F_i, M^G_j).

Second, all minutiae in sets M^F and M^G are transformed into their corresponding polar

systems referred to their central points, O_F and O_G, respectively. Let $V=\{V_{ij};\ |M^F|\geq i\geq 1\ |$

$M^G|\geq j\geq 1\}$ denote all similarities of aligned minutia pairs, where V_{ij} denotes that of M^F_i a

nd M^G_j, see Formula (9).

$$
\begin{cases}
V_{ij} = f\left(\Delta_{m_{ij}},diff\left(M^F_i,M^G_j\right)\right),\ if\ U_{ij}>0\\[2mm]
\Delta_{m_{ij}} = \left(\Delta_\alpha,\ ...,\ \Delta_\alpha,\ b(l_i/r_0,r_s,r_l),\ b(\alpha_0/l_i^2,\alpha_s,\alpha_l)\right)\\[2mm]
diff\left(M^F_i,M^G_j\right) = \left(...,\varphi^F_{ik}-\varphi^G_{jk}-\theta_m,...,\alpha^F_i-\alpha^G_j-\theta_m,\rho^F_i-\rho^G_j,\vartheta^F_i-\vartheta^G_j-\theta_m\right)
\end{cases}
\tag{9}
$$

If $V_{ij}\leq 0$, M^F_i and M^G_j are mismatched. In Formula (9), $b(x, x_0, x_1)$ is a step function p

roposed in the variably-sized bounding method [5] shown in Formula (10). The positional

parameters r_0, r_s, and r_l and direction parameters a_0, a_s, and a_l decide the size of the v

ariably-sized bounding box; $\left(\rho^F_i,\vartheta^F_i\right)$ and $\left(\rho^G_j,\vartheta^G_j\right)$ are the coordinates of M^F_i and M^G_j i

n polar systems respectively; $\Delta_{m_{ij}}$ is the vector of error thresholds of aligned minutia-pai

r M^F_i and M^G_j; and $diff(M^F_i, M^G_j)$ denotes the transformation-variant feature differences of M^F_i referred to M^G_j.

$$b(x, \ x_0, \ x_1) = \begin{cases} x_0 \ , & if \ \ x < x_0 \ ; \\ x \ , & if \ \ x_0 \leq x < x_1 \ ; \\ x_1 \ , & if \ \ x \geq x_1 \ ; \end{cases} \tag{10}$$

F   G

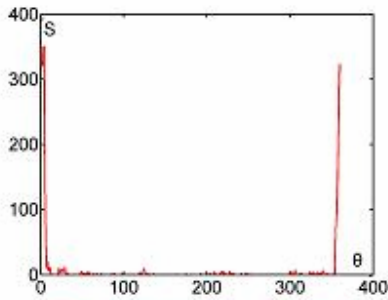**Figure 6. Fingerprints F and G acquired from the same finger with a sensor**

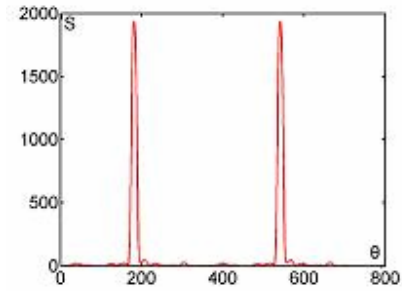**Figure 7. Distribution of comprehensive**

similarity *S* along rotation parameter *θ*

Figure 8. Filtered distribution of similar-

ity *S* along rotation parameter *θ*.
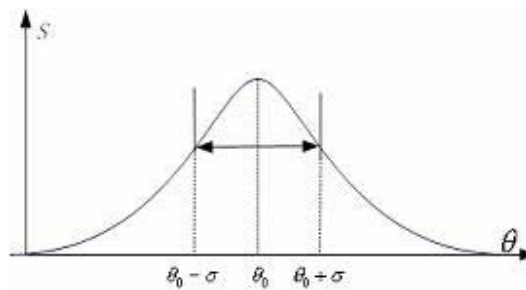
Figure 9. Rotation parameter calculated with geometric mean method from *H(S, θ)*

Finally, all local similarities in S is double-checked with Formula (9) in two cases. If $I_{mn}=1$, indicating that E^F_m and E^G_n match in positive order, S_{mn} is invalid when $V_{p^F_m p^G_n} \le 0$ and $V_{q^F_m q^G_n} \le 0$. If $I_{mn}=0$, indicating that E^F_m and E^G_n match in inverse order, S_{mn} is invalid when $V_{q^F_m p^G_n} \le 0$ and $V_{p^F_m q^G_n} \le 0$.

The revised local similarity set $S'= \{(S'_{mn}, I'_{mn}); |E^F|\ge i\ge 1, |E^G|\ge j\ge 1\}$ is performed as final matching step to measure the similarity between fingerprints F and G. $\sum_{S'_{mn},I'_{mn} \in S'} S'_{mn}$, $\sum_{V_{ij} \in V} V_{ij}$, $|S'|$, and $|V|$ are four final indices for global comprehensive similarity measurement between fingerprint F and G. They made it possible to judge whether two fingerprints come from the same finger in quantity. To reduce the effects of false local similarities in S on parameter estimation, θ_m is changed in the interval $[-1°, +1°]$ to make matching more robust. The above matching process is also looped three times to obtain an optimal team of performance indices $\sum_{S'_{mn},I'_{mn} \in S'} S'_{mn}$, $\sum_{V_{ij} \in V} V_{ij}$, $|S'|$, and $|V|$ as the final result in terms of the sum rule.

4. Results

Experiments were performed over the fingerprint databases provided by the 1st International Fingerprint Verification Competition in 2000 (FVC2000) [20] , 2nd International Fingerprint Verification Competition in 2002 (FVC2002) [25], and 3rd International Fingerprint Verification Competition in 2004 (FVC2004) [26]. Our experiments checked the validity of $H(S, \theta)$, analyzed of rotation parameter, and evaluated the final matching performance.

### 4.1. Validation of $H(S,\theta)$ in verification

Two sets of experiments were conducted to evaluate the performance of $H(S, \theta)$. 100 pairs of fingerprints were selected from different fingers. In the first group of 50 pairs, two fingerprints

in each pair were not similar as shown in Figures 10-a1 and 10-a2.   In the second group of 50

pairs, two fingerprints in each pair were similar, see Figures 11-a1 and 11-a2.   Figures 10-c and

11-c showed that the filtered $H(S, \theta)$ of a pair of fingerprints, selected either from the first group

or the second, has the characters as: 1) the comprehensive similarity is of random distribution

along the rotation parameter in a period, which is caused by mismatches produced by spurs or

deformation in fingerprints; 2) both the maximum and sum of $H(S,\theta)$ are small.   Compared with

the shape of Figure 10, that of Figure 11 is more regular because two fingerprints in Figures 11-

a1 and 11-a2 were more similar, which resulted in more local matches.

4.2. Validation of the rotation transformation parameter estimation

Two experiments were conducted to evaluate the performance of the $H(S, \theta)$ in rotation parame-

ter estimation and alignment.   The first experiment was performed over 20 fingerprints ran-

domly selected from twelve fingerprint databases of FVC2000, FVC2002 and FVC2004.   For

fingerprint F, its transformed fingerprint F' was produced by rotating F with an angle θ, which

changed from -15° to 15°, referred to its central point.   And rotation parameters θ' between F

and F' was estimated from their $H(S, \theta)$.   These results were shown in Figure 12.   The mean

and standard deviation of the absolute errors $|\theta - \theta'|$, were 0.42° and 0.26 respectively.

The second experiment was conducted to evaluate the global alignment of input minutiae with

the estimated rotation parameter. In this experiment, 50 groups of fingerprints were randomly

selected from the twelve fingerprint databases. Each group contained three fingerprints from the

same finger. For each group of fingerprints, as shown in Figures 13-a, 13-b, and 13-c, the minu-

tiae in the second and third fingerprints were mapped onto the first fingerprint with its corre-

sponding estimated rotation parameter θ_m, see Figure 13-c. Figure 14 illustrates the distribu-tion

of positional differences between aligned input minutiae and their corresponding template ones.
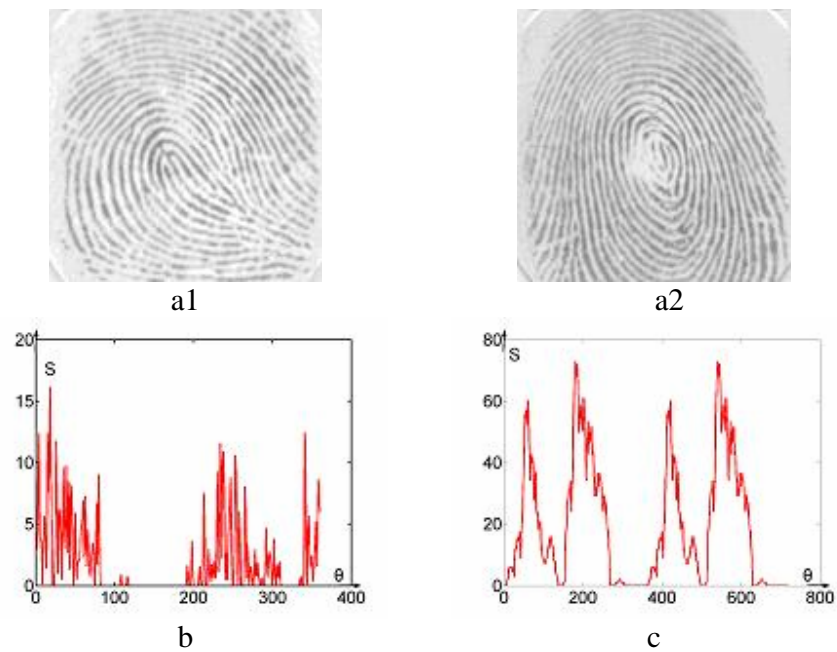
Figure 10. A pair of fingerprints selected from the first group and their *H(S, θ)*.

a1 and a2: two from two different fingers; b: their *H(S, θ)*; c: their Filtered *H(S,θ)*.
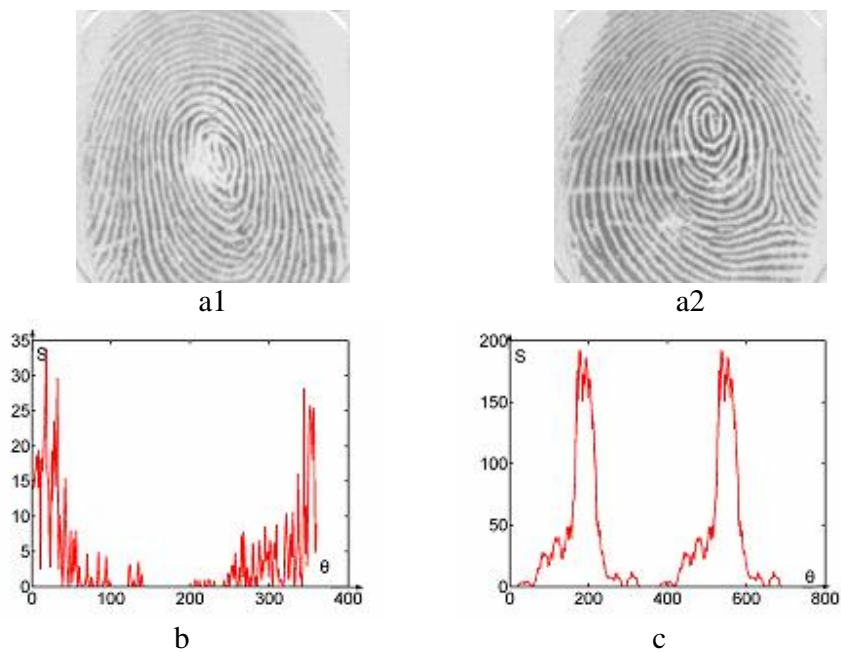
Figure 11. A pair of fingerprints selected from the second group and their *H(S, θ)*.

a1 and a2: two from two different fingers; b: their *H(S,θ)*; c: their Filtered *H(S,θ)*.

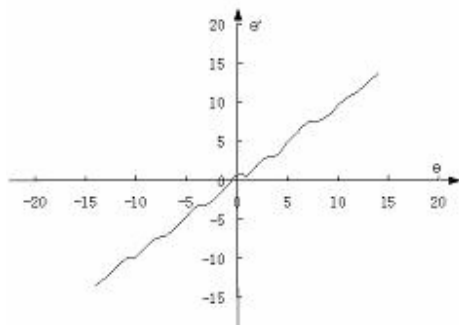**Figure 12. The distribution of rotation parameter biases between θ' and θ.**

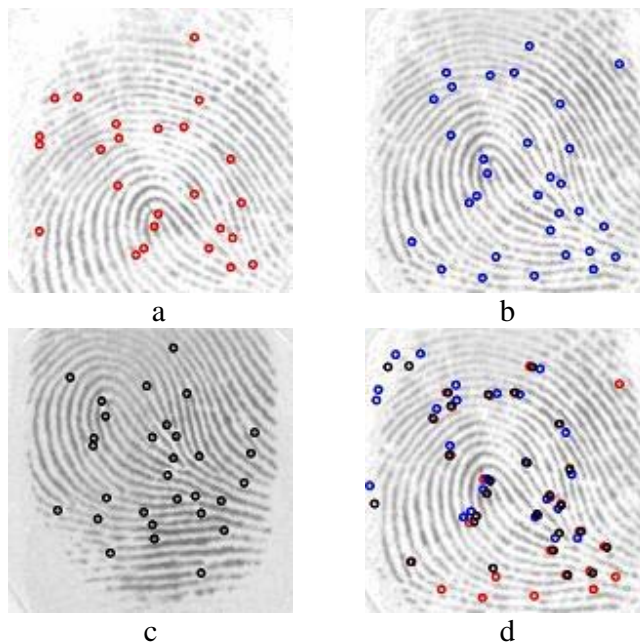a

b

c

d

Figure 13. Performance of the alignment. Minutiae in fingerprints b and c were

mapped onto fingerprint a respectively, see d.
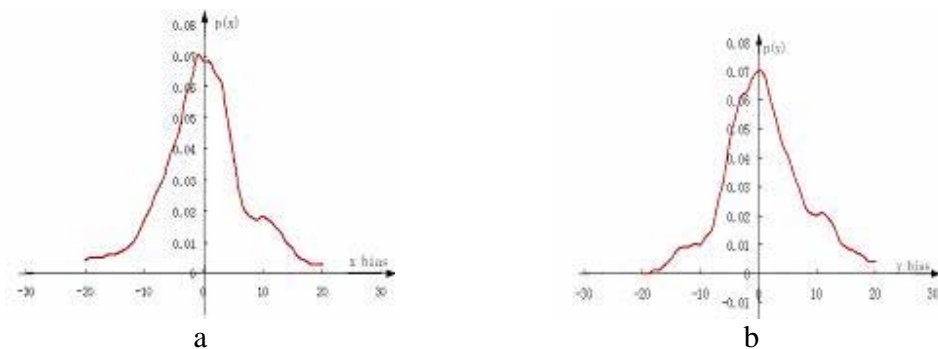

a

b

Figure 14. Distributions of position biases of aligned input minutiae to their cor-

responding template ones. a) Distribution of x biases; b) Distribution of y biases.

4.3. Matching performance analysis

To evaluate the overall matching performance of this method, a series of experiments were conducted over twelve fingerprint databases of FVC2000, FVC2002, and FVC2004, see Tables 1, 2, 3 and Figures 15, 16 and 17. In Figure 15, the four solid lines denoted Receiving Operating Curves (ROCs) drawn in log-log scales of this method over the four databases of FVC2000 respectively; the "+" lines denoted ones over the four databases of FVC2002; and "O" lines denoted ones over the four databases of FVC2004. Tables 1, 2, and 3 described the performance of this method over the twelve databases with some performance indices provided by FVC2000 and FVC2002. This new method obviously outperformed the previous work, variably-bounded box-based matching method [5], see Figure 16. In the two methods, the same fingerprint enhancement method, Cheng's dyadic scale space-based fingerprint enhancement method [19] and Luo's knowledge-based post-processing method [17] were applied for fingerprint pre-processing and comprehensive minutia detection were employed in matching. Their performance evaluated over DB1_A of FVC2000 demonstrated the effectiveness of the new matching method.

To judge whether ridge-based feature and ridge information were helpful for fingerprint matching, the method without ridge-based relative features nor ridge information, denoted by GCS_NN, was compared with the method which having only ridge information called as GCS_NR, and the method with ridge-based relative features and ridge information, called as GCS_GR over the four fingerprint databases DB1_a of FVC2002, DB1_a, Db2_a, and DB4_a of 2004 respectively. Among the twelve fingerprint databases of FVC2000, FVC2002, and FVC2004, the overall fingerprint quality of DB1_a and Db2_a of 2004 is the worst while DB1_a of FVC2002 and DB4_a of FVC2004 are the better databases. The differences among the four fingerprint databases illustrated by Figure 17 and Table 4 approved that ridge-based relative fea-

tures and ridge information were available in fingerprint matching, and those features help decrease the scores of impostor matches.   For example, there is a step jump at FMR close to -4 of ROC, such as line "o" in Figure 17(b), if the scores of impostor matches are too great.

We noted that our method outperformed Tico's matching method with an orientation-based minutia descriptor[14] over the 1st and 2nd databases of FVC2000 and the Teoh's matching method with integrated wavelet and Fourier-Mellin invariant transformation[10] over the four databases of FVC2002. The good performance of GCS_GR over the databases of FVC2000, FVC2002 and FVC2004 were contributed by the following aspects: 1) minutia was replaced by minutia-simplex, and minutia-simplex had more relative features to represent a fingerprint; 2) the ridge-based nearest neighbourhood among minutiae was employed to check coarse matching; 3) the rotation parameter was calculated in term of histogram.

Table 1.   Results of our new method over the four databases of FVC2000

Database (FVC2000)	EER (%)	EER* (%)	ZeroFMR (%)	ZeroFNMR (%)	Rej_Match (%)	Rej_Enroll (%)	AE&MT (S)
DB1_a	1. 79	1. 79	4.39	100	0.000	0.000	0.82
DB2_a	0.99	0.99	2.49	100	0.000	0.000	1.10
DB3_a	3.54	3.54	9.74	100	0.000	0.000	0.85
DB4_a	1.64	1.64	5.05	100	0.000	0.000	0.87

Table 2.   Results of our new method over the four databases of FVC2002

Database (FVC2002)	EER (%)	FMR100 (%)	FMR1000 (%)	ZeroFMR (%)	Rej_Match (%)	Rej_Enroll (%)	AE&MT (S)
DB1_a	1.963	2.500	4.000	5.036	0.000	0.000	0.83
DB2_a	1.110	1.250	1.964	4.286	0.000	0.000	1.20
DB3_a	4.312	7.143	10.250	13.107	0.000	0.000	0.73
DB4_a	2.772	3.429	6.071	7.679	0.000	0.000	0.83

Table 3.   Results of our new method over the four databases of FVC2004

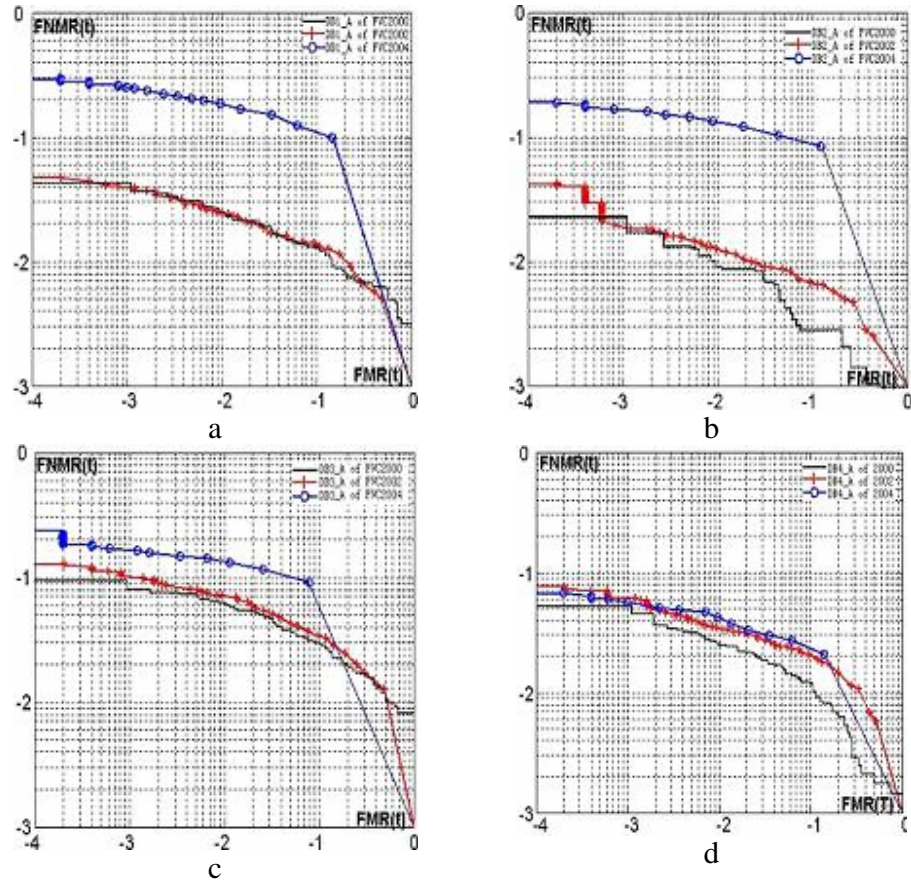| Database (FVC2004)	EER (%)	FMR100 (%)	FMR1000 (%)	ZeroFMR (%)	Rej_Match (%)	Rej_Enroll (%)	AE&MT (S)
DB1_a	9.335	18.500	25.036	30.286	0.000	0.000	0.81
DB2_a	7.345	13.393	16.607	19.893	0.000	0.000	0.76
DB3_a	8.529	13.107	16.536	22.536	0.000	0.000	1.02
DB4_a	2.719	4.214	5.571	7.000	0.000	0.000	0.78

Figure 15. ROCs (drawn in log-log scales) of our new method over the twelve databases of FVC2000, FVC2002, and FVC2004 respectively.
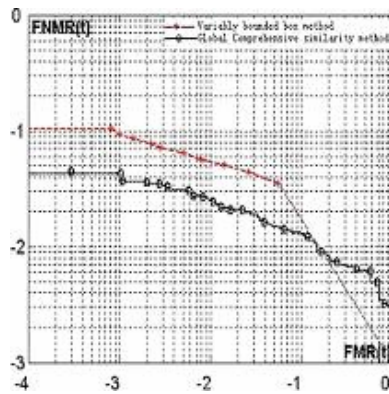

Figure 16. Performance difference between the variably bounded box method and the new method over DB1_a of FVC2000. The "*" line and the "o" line denote their ROCs (drawn in log-log scales) over the database respectively.

Table 4. Performance differences among GCS_NN, GCS_NR and GCS_GR over four

databases

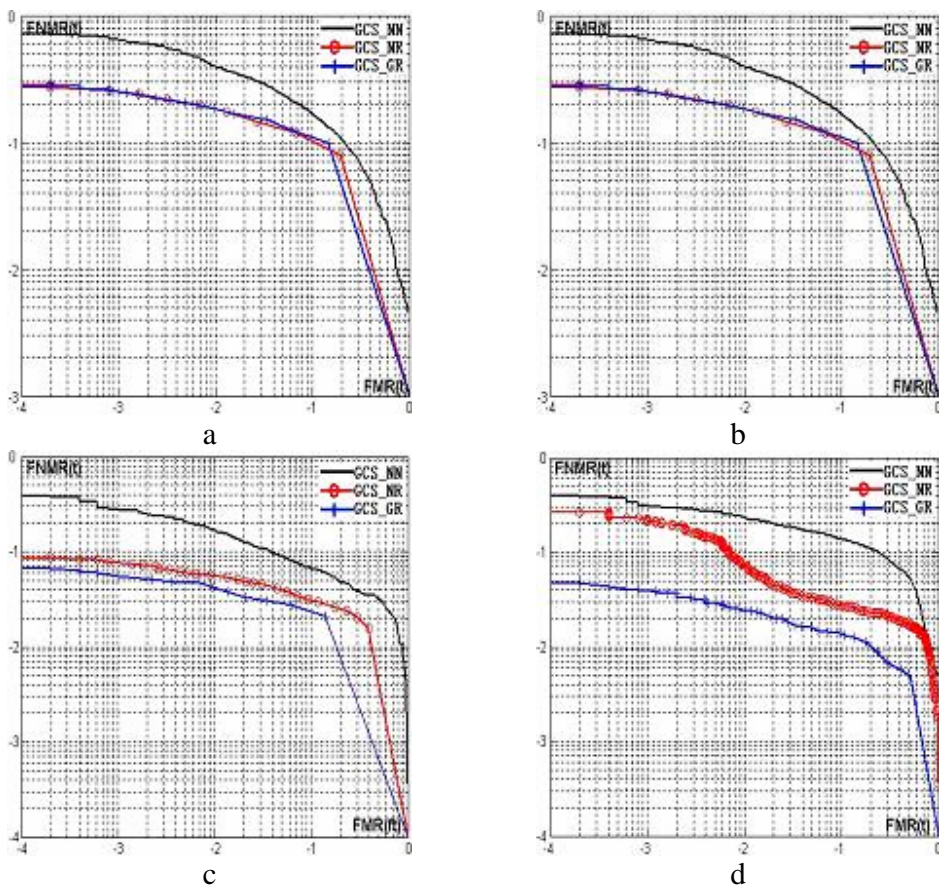| Database	EER of GCS_NN(%)	EER of GCS_NR(%)	EER of GCS_GR(%)
DB1_a of FVC2004	13.707	10.028	9.335
DB2_a of FVC2004	12.773	8.876	7.345
DB4_a of FVC2004	7.432	3.813	2.719
DB1_a of FVC2002	3.528	2.363	1.963
Average of |EER of GCS_NR - EER of GCS_NN|: 3.090			
Average of |EER of GCS_GR - EER of GCS_NR|: 0.930			

a

b

c

d

Figure 17.Performance differences among GCS_NN, GCS_NR, and GCS_GR over

four databases. a) Performance difference over DB1_a of FVC2004; b) perform-

ance difference over DB2_a of FVC2004; c) performance difference over DB4_a of

FVC2004; d) their performance difference over DB1_a of FVC2002.

4.4. Template Size Analysis

In our method, the memory expense of a comprehensive minutia depicted by a minutiae and its associate ridge information is 8 bytes if T, the number of sampled points along a ridge skeleton, is set to 2. T can be reasonably modified according to the memory requirement of an AFIS. Empirically, the average memory expense used to present ridge-based nearest neighbourhood is no more than 4.5 bytes. Therefore, the mean memory expense is 12.5 bytes for a comprehensive minutiae representation. Minutia-simplexes don't influence the memory expense for storage.

The number of minutiae varies in different fingerprints but a good one contains 60-80 minutiae [9]. Assuming there are 80 minutiae in a fingerprint, then1000 bytes is more than enough for a fingerprint presentation. In different methods, template size varies. For a method based on comprehensive feature composing of minutiae and ridge information, its template size is generally more than 1k bytes. For example, for Jain's hybrid fingerprint method [13] and Tico's orientation–based minutia descriptor [14], more than 1k bytes is required to describe the features of a fingerprint. For methods based on global features, their template sizes may be larger, such as Sujan's space invariant transforms based fingerprint identification method [11] . For methods using only minutiae, such as Gold's graph matching method [4], their template sizes are no more than 500 bytes, but their performance is compromised.

5. Conclusion, discussion and further work

A new fingerprint matching method based on global comprehensive similarity is introduced in this paper with two novel techniques. First, a minutia-simplex and the ridge-based nearest neighbourhood among minutiae are performed to represent two relative structures among minutiae in different directions. Second, $H(S, \theta)$ is defined to model the relationship between transformation parameters and comprehensive similarity in terms of histogram. From this histo-

gram, an optimal rotation parameter is estimated for alignment. Our method works well over the fingerprint databases of FVC2000, FVC2002 and FVC2004, and it can be applied to a memory-limited AFIS owing to its less than 1k byte template size. However, this method is sensitive to the quality of the fingerprint. The quality of fingerprints affects the reliability of minutiae, rotation parameter, center points, and therefore affects matching performance. As shown in Figure 17(a), the ridge-based relative feature has limited ability to improve fingerprint matching performance in bad-quality fingerprints. For example, 99_5.tif in the DB2_a of FVC2004 is a bad-quality fingerprint with no more than four genuine minutiae detected in our method. In another case, 85_1.tif and 85_8.tif in DB1_a of FVC2004 have a small common region of good quality. As a result, less than three genuine minutiae are matched.

We will continue our investigations to improve the method in minimizing false match, which occasionally occurs under the condition of large deformation in fingerprints and very poor-quality fingerprints. Based on Chen's registration pattern inspection method [27], the adaptive matching template will be tested in fingerprint matching to reduce the impacts of deformation in a fingerprint. Global pattern and features, as well as a hybrid matching technique will be investigated to reduce the sensitivity of poor quality fingerprint. Additionally, we will study the technique that employs a multi-resolution search strategy to calculate the optimal transformation.

Appendix Threshold Estimation

In proposed method, the thresholds, i.e., Δ_l, Δ_α, Δ_β (the error thresholds of distance, direction and grey variance of a minutia-simplex), L_l and L_h (the lower and upper bounds of the distant attribute in a valid minutia-simplex), are estimated from a training fingerprint dataset that consists of N pairs of fingerprints with the following steps.

Step 1. Build a set of transformation-irrelevant feature offset vectors of minutiae-simplex. For each pair of fingerprints, F_k and G_k, label their corresponding minutia pairs and push them into set $\{(M_i^{F_k}, M_i^{G_k})\}$; then randomly select two minutia pairs $(M_i^{F_k}, M_i^{G_k})$ and $(M_j^{F_k}, M_j^{G_k})$ from set $\{(M_i^{F_k}, M_i^{G_k})\}$ to build two minutia-simplexes $E_m^{F_k}$ and $E_m^{G_k}$ without distant constraint; and then compare the transformation-irrelevant features of $E_m^{F_k}$ and $E_m^{G_k}$ to get the offsets described by vector $(d_m, dl_m, d\alpha_m, d\beta_m)$, where $d_m = \min\{l_m^{F_k}, l_m^{G_k}\}$, $d\alpha_m = \left(\left|u_m^{F_k} - u_m^{G_k}\right| + \left|v_m^{F_k} - v_m^{G_k}\right|\right)/2$, $dl_m = \left|l_m^{F_k} - l_m^{G_k}\right|$, and $d\beta_m = \left(\left|\beta_i^{F_k} - \beta_i^{G_k}\right| + \left|\beta_j^{F_k} - \beta_j^{G_k}\right|\right)/2$; finally put the vector into offset vector set D_k. All combinations of two elements out of the set $\{(M_i^{F_k}, M_i^{G_k})\}$ are used to create offset vectors and added into set D_k.

All pairs of fingerprint are examined by the same method to produce the corresponding offset vector sets D_k ($N \geq k \geq 1$). These sets are united as $D = D_1 \cup D_2 \cup \ldots \cup D_N$.

Step 2. Estimate thresholds Δ_l, Δ_α, and Δ_β. Histograms of dl, $d\alpha$ and $d\beta$ built with set D are denoted as $H_{dl}(dl)$, $H_\alpha(d\alpha)$ and $H_{d\beta}(d\beta)$ respectively. According to these histograms, thresholds Δ_l, Δ_α, Δ_β and their corresponding threshold space $T = \{(dl, d\alpha, d\beta) \mid dl \leq \Delta_l; d\alpha \leq \Delta_\alpha; d\beta \leq \Delta_\beta\}$ are calculated when $\frac{|D'|}{|D|} \geq \eta_1$, where $D' = \{(d_m, dl_m, d\alpha_m, d\beta_m) \mid (dl_m, d\alpha_m, d\beta_m) \in T\}$.

Step 3. Estimate the lower and upper bounds of the distant feature of a minutia-simplex. First, build the histogram of the distant feature of minutia-simplex, called as $H_d(d)$ with set D'; then find d_o and an interval $[L_l, L_h]$ on the condition that $H_d(L_l) = H_d(L_h)$, $\frac{|D''|}{|D'|} \geq \eta_2$, $H_d(d_o) = \max\{H_d(d)\}(L_h \geq d_o \geq L_l)$, where

$D'' = \{D''_m = (d_m, dl_m, d\alpha_m, d\beta_m)\,|\,D''_m \in D \text{ and } d_m \in [L_l, L_h]\}$. Statistically, if $|D'|$ is enough large, $H_d(d)$ is of normal distribution. In threshold estimation, both η_1 and η_2 are so great that set D'' has enough elements, representing the differences among minutia-simplex pairs, to calculate the similarity between two fingerprints.

Acknowledgements

References

[1] S. Z. Li, *Markov Random Field Modeling In Image Analysis*. Springer-Verlag, 2001.

[2] X.D. Jiang and W.Y. Yau, "Fingerprint Minutiae Matching Based on the Local and Global Structures," *Proc. 15th Int. Conf. Pattern Recognition*, Vol. 2, pp.1038-1041, 2000.

[3] B. Bhanu and X.J. Tan, "Fingerprint Indexing Based on Novel Features of Minutiae Triplets," *IEEE Trans. Pattern Analysis and Machine Intelligence*, Vol.25, No.5, pp.616 – 622, May 2003.

[4] S. Gold and A. Rangarajan, "A Graduated Assignment Algorithm for Graph Matching," *IEEE Trans. Pattern Analysis and Machine Intelligence,* Vol.18, No.4, pp.377-388, Apr. 1996.

[5] Y.L. He, J. Tian, X.P. Luo, and T.H. Zhang, "Image Enhancement and Minutiae Matching in Fingerprint Verification," Pattern Recognition Letters, Vol. 24/9-10 pp.1349 -1360, 2003.

[6] D. Maltoni, D. Maio, A.K. Jain and S. Prabhakar, Handbook of Fingerprint Recognition. Springer- Verlag, 2003.

[7] A.K. Jain, S. Pankanti, and H. Lin, "A Multichannel Approach to Fingerprint Classification," *IEEE Trans. Pattern Analysis and Machine Intelligence*, Vol. 21, No. 4, pp. 348-359, Apr. 1999.

[8] J.H. Chang and K.Ch. Fan, "A New Model for Fingerprint Classification by Ridge Distribution Sequences," *Pattern Recognition*, Vol.35, No.6, pp.1209-1223, Jun. 2002.

[9] A. K. Jain, S. Prabhakar, L. Hong, and S. Pankanti, "Filterbank-Based Fingerprint Matching," *IEEE Trans. Image Processing*, Vol.9, No.5, pp.846-859, May 2000.

[10] A. Teoh, D. Ngo, O. T. Song, "An Efficient Fingerprint Verification System Using Integrated Wavelet and Fourier–Mellin Invariant Transform," *Image and Vision Computing*, Vol.22, No.6, pp.503–513, Jun. 2004.

[11] V.A. Sujan and M.P. Mulqueen, "Fingerprint Identification Using Space Invariant Transforms," *Pattern Recognition Letters*, Vol.23, No.5, pp.609–619, Mar. 2002.

[12] C.J. Lee and S.D. Wang, "Fingerprint Feature Reduction by Principal Gabor Basis Function," *Pattern Recognition*, Vol.34, No.11, pp.2245-2248, Nov. 2001.

[13] A. Ross, A.K. Jain, and J. Reisman, "A Hybrid Fingerprint Matcher," *Pattern Recognition*, Vol.36, No.7, pp.1661–1673, Jul. 2003.

[14] M. Tico and P. Kuosmanen, "Fingerprint Matching Using an Orientation-Based Minutia Descriptor," *IEEE Trans. Pattern Analysis and Machine Intelligence*, Vol.25, No.8, pp.1009-1014, Aug. 2003.

[15] A.K. Jain, A. Ross, and S. Prabhakar, "Fingerprint Matching Using Minutiae and Texture Features," *Proc. 2001 Int. Conf. Image Processing*, Vol.3, pp.282-285, 2001.

[16] T.H. Zhang, J. Tian, Y.L. He, and X. Yang, "Fingerprint Alignment Using Similarity Histogram," Proc. 4th Int. Conf. Audio and Video-based Biometric Person Authentication, pp.854-861, 2003.

[17] X.P. Luo and J. Tian, "Knowledge Based Fingerprint Image Enhancement," *Proc. 15th Int. Conf. Pattern Recognition*, Vol.4, pp.783-786, 2000.

[18] Q.H. Xiao and H. Raafat, "Fingerprint Image Post-processing: A Combined Statistical and Structural Approach," *Pattern Recognition*, Vol.24, No.10, pp.985-992, Oct.1991.

[19] J.G Cheng and J. Tian, "Fingerprint enhancement with dyadic scale-space," Pattern Recognition Letters, Vol.25, pp.1273-1284, 2004.

[20] D. Maio, D. Maltoni, R. Cappelli, J.L. Wayman and A.K.Jain, "FVC2000: Fingerprint Verification Competition," *IEEE Trans. Pattern Analysis and Machine Intelligence*, Vol.24, No.3, pp.402-412, Mar. 2002.

[21] K.A. Toh, W.Y. Yau, X.D Jiang, and et al, "Minutiae Data Synthesis for Fingerprint Identification Applications," *Proc. 2001 Int. Conf. Image Processing*, Vol.2, pp.262-265,

[22] 2000. Cappelli, D. Maio, and D. Maltoni, "Modelling Plastic Distortion in Fingerprint Images," *Proc. 2nd Conf. Advances in Pattern Recognition*, 2001.

[23] A.M. Bazen and S. H. Gerez, "Elastic Minutiae Matching by Means of Thin-Plate Spline Models," *Proc. 16th Int. Conf. Pattern Recognition,* Vol.2, pp.985-988, 2002.

[24] A. Senior and R. Bolle, "Improved Fingerprint Matching by Distortion Removal," *IEICE Trans. Information and Systems, Special issue on Biometrics*, Vol. E84-D, No.7, pp.825-831, Jul. 2001.

[25] D. Maio, D. Maltoni, R. Cappelli, J.L. Wayman, and A.K. Jain, "FVC2002: Second Fingerprint Verification Competition," *Proc.16th Int. Conf. Pattern Recognition,* Vol.3, pp.811-814, 2002.

[26] D. Maio, D. Maltoni, R. Cappelli, J. L. Wayman and A. K. Jain, "FVC2004: Third Fingerprint Verification Competition," *Proc. 1st Int. Conf. Biometric Authentication*, pp.1-7, Jul. 2004.

[27] H. Chen, J. Tian, and X. Yang, "Fingerprint Matching with Registration Pattern Inspection," *Proc. 4th Int. Conf. Audio and Video-based Biometric Person Authentication*, pp.327-334, 2003.